Representation of odorants by receptor neuron input to the mouse olfactory bulb

Matt Wachowiak and Lawrence B. Cohen

Dept. Cellular and Molecular Physiology, Yale University School of Medicine, New Haven, CT 06520
Marine Biological Laboratory, Woods Hole, MA 02543

Running Title: Receptor neuron input to the mouse olfactory bulb

Address for correspondence:

Matt Wachowiak
Dept. Cellular and Molecular Physiology
Yale University School of Medicine
333 Cedar St.
New Haven CT 06520

matt.wachowiak@yale.edu
Ph: (203) 785 – 4047
Fax: (203) 785 - 6871

Summary

To visualize odorant representations by receptor neuron input to the mouse olfactory bulb, we loaded olfactory receptor neurons with a calcium-sensitive dye and imaged odorant-evoked fluorescence increases from their axon terminals *in vivo*. Optical signals reflected activation of receptor neuron populations converging onto individual glomeruli. We report several new findings. First, five glomeruli were identifiable across animals based on their location and response to one or two odorants; all five showed complex response specificities. Second, maps of receptor neuron input were chemotopically organized at near-threshold concentrations but, at moderate concentrations, involved many, widely distributed glomeruli. Third, the dynamic range of input to a glomerulus was greater than that reported for individual receptor neurons. Finally, odorant activation slopes differed across glomeruli and, sometimes, for different odorants activating the same glomerulus. These results suggest a high degree of complexity in odorant representations at the level of input to the olfactory bulb.

Introduction

Animals use olfactory information in a wide variety of behavioral tasks. Spatially-organized patterns of neuronal activity in the CNS have long been hypothesized to play an important role in representing olfactory information (Adrian, 1953; Kauer, 1991; Shepherd, 1994). This hypothesis is strongly supported by studies imaging neuronal activity in the vertebrate olfactory bulb (Stewart et al., 1979; Guthrie et al., 1993; Friedrich and Korsching, 1997; Johnson et al., 1998; Rubin and Katz, 1999; Uchida et al., 2000; Xu et al., 2000; Meister and Bonhoeffer, 2001) and in its insect analog, the antennal lobe (Sachse et al., 1999). Thus, a fundamental step in olfactory coding appears to involve the transformation of an odorant's molecular features into a spatial map of neuronal activity.

The molecular and anatomical basis for this transformation has been extensively studied in the mouse. Here, most olfactory receptor neurons express one out of ~1000 olfactory receptor proteins (Malnic et al., 1999; Rawson et al., 2000), each of which is thought to bind odorants with particular molecular features. All of the 10,000 – 20,000 neurons expressing the same receptor protein converge onto a few (1 - 3) glomeruli in stereotyped locations of the olfactory bulb (Vassar et al., 1994; Mombaerts et al., 1996; Strotmann et al., 2000). Thus, odorant-evoked activity of receptor neurons distributed across the olfactory epithelium is transformed into a spatially-organized pattern of input to olfactory bulb glomeruli. This map of input is likely further transformed by synaptic processing within and between glomeruli as olfactory information is transferred to second-order (output) neurons in the olfactory bulb (Yokoi et al., 1995).

While odorant response properties of single receptor neurons have been well characterized, the response properties expressed by a population of neurons converging onto a glomerulus may be different. For example, the dynamic range of single receptor neurons typically spans ~1 log unit of concentration (Firestein et al., 1993; Trotier, 1994; Reisert and Matthews, 2001), but differences in sensitivity across a population of convergent neurons could result in a larger dynamic range at the level of glomerular input (Firestein et al., 1993; Cleland and Linster, 1999). Such population-level response properties may be important determinants of odorant representations.

While functional imaging methods effectively reveal patterns of glomerular activity, with many of thse methods it is difficult to relate the signals to a particular class of neurons. In contrast, labeling neurons with voltage- or calcium-sensitive dyes via retrograde or anterograde transport allows selective monitoring of activity in defined neuronal populations (e.g., O'Donovan et al., 1993; Tsau et al., 1996; Kreitzer et al., 2000). In the zebrafish and the turtle, voltage-and calcium-sensitive tracer dyes applied to the olfactory epithelium have enabled imaging of population-level receptor neuron input to the olfactory bulb (Friedrich and Korsching, 1997; Friedrich and Korsching, 1998; Wachowiak et al., 2000b). Interpretation of these results, however, is limited because single glomeruli in these animals are difficult to resolve, and because little is known about the molecular and anatomical organization of receptor neuron projections to olfactory bulb glomeruli.

We have used calcium-sensitive dyes to image receptor neuron activity from the dorsal olfactory bulb of the mouse with a spatial resolution sufficient to resolve

individual glomeruli and a temporal resolution of 40 ms. We investigated the specificity, chemotopy, and concentration-dependence of receptor neuron input to glomeruli, and report several novel findings. First, individual glomeruli can be identified across animals based on their location and primary response characteristics, and all of these glomeruli show complex response specificities. Second, while near-threshold odorant concentrations evoke input to a few glomeruli in a broadly chemotopic fashion, slightly higher concentrations evoke input to many glomeruli distributed widely across the dorsal bulb. Finally, we report that the concentration-response function of input to a single glomerulus shows a wider dynamic range than that reported for single neurons, differs significantly across glomeruli, and can differ for different odorants activating the same glomerulus. These results suggest that odorant representations are broadly distributed across many glomeruli, show complex changes with concentration, and that some features of odorant representations are emergent properties that arise from the convergence of many receptor neurons onto a single glomerulus.

Results

Olfactory receptor neuron loading and imaging

Calcium Green-dextran loading (adapted from Friedrich and Korsching, 1997) resulted in olfactory receptor neuron labeling throughout the olfactory epithelium. In 10 mice we investigated the time-course of transport to the olfactory bulb and the effect of loading on olfactory receptor neuron responses. Labeling in olfactory receptor axon terminals in the olfactory bulb was evident after 24 hrs and increased in intensity over the next 48 hrs, at which point many glomeruli were strongly labeled (Figures 1A, B). Labeling remained strong for at least 8 days, and, in the bulb, was specific to olfactory receptor neurons. The loading procedure caused an immediate decrement in the responsiveness of olfactory receptor neurons to odorants, as measured by electroolfactogram (EOG) recordings from the olfactory epithelium, presumably reflecting the loss of cilia from olfactory receptor neurons (Adamek et al., 1984; Friedrich and Korsching, 1997). However, after 48 hrs, the EOG amplitude was indistinguishable from that of untreated epithelia (not shown).

We imaged odorant responses from the dorsal olfactory bulb of anesthetized mice 4 - 8 days after loading. Odorant presentation evoked rapid (200 - 500 ms rise-time) increases in fluorescence of up to 6% $\Delta F/F$ (Figures 1C, F). Signals were easily detected in single trials. Spatial maps of the response amplitude measured from each pixel showed well-defined foci of fluorescence increases (Figures 1D, E), often corresponding to individual glomeruli visible from the resting fluorescence (Figure 1B). Amplitude profiles through these glomerular signals were well-fit by a Gaussian function with $\sigma = 38 \pm 9$ μm (mean ± s.e.m.; n = 101), corresponding to a full-width at half-maximum of 89 μm. Diffuse, non-localized signals with the same time-course as the odorant-evoked signals were also observed, possibly due to scattered or out-of-focus light. Odorant-evoked signals showed a range of amplitudes in different glomeruli (Figure 1D, inset). The spatial distribution and amplitude of the signals was consistent across repeated odorant presentations and was different for different odorants (Figures 1D, E, F). With many trials

(> 100) over long time intervals (several hours), the response amplitudes declined but the spatial patterns remained constant.

Previous experiments using this imaging method in the zebrafish and turtle olfactory bulbs showed that Calcium Green fluorescence increases reflect action potential-evoked calcium influx into receptor neuron axon terminals (Friedrich and Korsching, 1997; Wachowiak and Cohen, 1999). This signal thus reflects activation of the population of 10 – 20,000 receptor neurons innervating each glomerulus.

We imaged odorant-evoked input to dorsal glomeruli in 35 olfactory bulbs from 30 mice, using odorants known to activate dorsal glomeruli in rodents (Bozza and Kauer, 1998; Rubin and Katz, 1999; Johnson and Leon, 2000; Uchida et al., 2000). In experiments evaluating chemotopy and recruitment of glomeruli, responses were imaged across most of the dorsal bulb at 10.5x magnification, with a field of view of 1.7 mm x 1.7 mm. Subsequent histological analyses (*en bloc* Sudan Black staining; Lamantia et al., 1992) from 10 imaged preparations indicated that this region included approximately 150 glomeruli. In other experiments, responses were imaged at 14x (1.3 mm x 1.3 mm field of view).

Chemotopic organization of receptor neuron input

At near-threshold concentrations (0.02% - 0.4% dilution of saturated vapor), odorants activated only a few (1 - 9) glomeruli. Odorants with different functional groups preferentially activated glomeruli in different regions of the dorsal bulb (Figure 2A). Figure 2B shows locations of glomeruli activated by odorants from five structural classes, compiled across 12 preparations and aligned relative to the intersection of the midline and the caudal sinus. Aliphatic aldehydes and fatty acids preferentially activated anteromedial glomeruli, while ketones and acetates preferentially activated caudal-lateral glomeruli (Figure 2B). Benzaldehyde activated caudal-lateral as well as central and medial glomeruli. Odorants with the same functional group, but different carbon chain length, activated glomeruli in the same region of the bulb, with no clear relationship between glomerular location and carbon chain length, as shown for a series of aldehydes (C3, C6 and C8) in Figure 2C. Similar results were observed in five additional preparations tested with aldehydes differing by at least two carbons (C4 - C8), five with ketones (C4 and C6), and three with acetates (C3 - C6). In addition, Figure 2C shows that aldehydes with a chain length differing by as much as 5 carbons evoke input to a number of the same glomeruli. Figure 2C also shows that the fatty acid hexanoic acid evokes input to many of the same glomeruli as the aldehydes.

Effect of concentration on odorant representations

Increasing odorant concentrations moderately above threshold recruited input to many additional glomeruli. For example, Figure 3A shows responses to 0.1% (a near-threshold concentration) and 1.9% hexanal, imaged from the anterior 3/4 of the dorsal bulb at 14x magnification. There is an approximately four-fold increase in the number of activated glomeruli, with glomeruli activated across most of the imaged area. Significant recruitment was seen for all odorants tested at suprathreshold concentrations (aldehydes, ketones, acetates and benzaldehyde) and in all preparations. For odorants tested at both

near-threshold (0.1 - 0.4%) and 5- to 10-fold higher concentrations (1 - 2% dilution), the mean number of activated glomeruli across the dorsal surface increased from 6 ± 1 to 19 ± 2 (n = 33 concentration pairs). Hexanal and the ketones 2-butanone and 2-hexanone showed the most recruitment, with the number of glomeruli increasing from 7 ± 1 to 22 ± 3 (n = 10) for hexanal, and from 8 ± 1 to 34 ± 7 (n = 6) for the ketones. In some trials, odorants activated as many as 30 - 60 glomeruli. This recruitment was not due to an increase in the signal-to-noise ratio of the response, because increasing the number of averaged trials from 4 to 32 did not increase the number of glomeruli apparent at low concentrations. In three preparations, each tested with 1 - 2% dilutions of an aldehyde, an acetate, and a ketone, we counted 67, 68 and 99 distinct activated glomeruli. These numbers constitute a substantial fraction of the total number of glomeruli (~150) estimated to be present in the the imaged region.

Intrinsic imaging studies have reported fewer glomeruli activated by comparable concentrations of the same odorants (Belluscio and Katz 2001; Meister and Bonhoeffer 2001). These studies spatially filtered or thresholded the signal images before counting glomeruli. To test whether either kind of processing might affect the number of detected glomeruli, Figure 3B shows the response to 1.9% hexanal (from Figure 3A) after smoothing with a Gaussian kernel and subtracting the smoothed data (Meister and Bonhoeffer 2001), and Figure 3C shows the same response after thresholding the data at two standard deviations above the mean (Belluscio and Katz 2001) (Figure 3C). High-pass filtering preserves nearly all of the glomeruli visible in the unfiltered image. However, thresholding the data eliminates many of the glomeruli.

Suprathreshold odorant concentrations activated glomeruli outside of the domains observed at near-threshold concentrations. Figure 3D shows the locations of glomeruli activated by 1 - 2% dilutions of hexanal, hexyl acetate, the ketones 2-butanone and 2-hexanone (combined), and benzaldehyde, imaged from multiple preparations and aligned as in Figure 2B. All odorants activate glomeruli across much of the dorsal surface. Increasing concentration caused an increase in the number of glomeruli activated by more than one odorant. However, response maps evoked by different odorants remained distinct, even at concentrations five- to ten-fold higher than those used in Figure 3D. For example, Figure 3E shows responses to 2-hexanone, imaged from the caudal 3/4 of the dorsal bulb over a 165-fold concentration range, with many (33) glomeruli activated at 11% dilution. The two glomeruli marked by arrows in Figure 3E are recruited by 0.25% hexanone (Figure 3E), but the structurally similar 2-butanone fails to activate these glomeruli (Figure 3F) even at 11% dilution, which corresponds to a molar vapor concentration 360 times greater than that of 0.25% hexanone. This result was generally true: in all tested cases, response maps evoked by different odorants remained distinct at all concentrations tested. Thus, odorant representations maintain specificity over a large concentration range.

Functional and topographic identification of glomeruli

Near-threshold concentrations of some odorants consistently activated glomeruli in the same location in multiple preparations, suggesting that glomeruli could be identified across animals. Five such glomeruli (designated A through E) are shown in Figure 4A. Each of these glomeruli were one of only a few glomeruli activated at near-

threshold concentrations of a particular odorant (hexanal for glomerulus A; hexyl acetate for glomeruli B and C; benzaldehyde for glomeruli D and E) and each was often the only glomerulus activated in a particular region. Figure 4B shows the locations of glomeruli A through E identified in a number of preparations and aligned as described above. Each glomerulus is found within a restricted area. Ease of identification was somewhat dependent on glomerulus location (i.e. - glomerulus C was difficult to identify because of its far rostral and lateral position, which was often out of focus), but 4 of the 5 glomeruli were identified in the majority of preparations (see Figure 4 legend).

While each glomerulus was identified based on its response to one or, occasionally, two, odorants, the response spectrum of each identified glomerulus to a panel of additional odorants was consistent across animals. As a partial example, Figure 4C shows the response of glomerulus A to four odorants tested in five animals, with consistent responses to hexanal and hexanoic acid, but not to hexyl acetate or 2-hexanone. We determined the relative sensitivity of each glomerulus to a panel of 16 odorants by compiling responses across preparations (Figure 5). For each glomerulus, we first measured the response to a near-threshold concentration of the 'primary' odorant used to identify that glomerulus. The relative sensitivity to a 'test' odorant, was determined by dividing the concentration of the primary odorant by the lowest concentration of the test odorant that evoked a similar-amplitude response. For odorants tested in multiple preparations, the relative sensitivities were averaged; however, this value varied little across preparations. Odorants that failed to evoke any response in a glomerulus at the highest concentrations tested were assigned a relative sensitivity value of <0.1 (note that this group also includes odorants that did activate the glomerulus but at $>$ 10-fold higher concentrations than the primary odorant).

All five glomeruli showed complex, but different, relative sensitivity profiles (Figure 5). Glomerulus A was selective for C5 - C8 aldehydes, but was equally sensitive to C5 and C6 fatty acids. Glomerulus B was selective for C4 to C8 acetates, but was also moderately sensitive to octanal, benzaldehyde, hexanol and 2-hexanone. In contrast, glomerulus C was not selective for acetate chain length (C3 - C8) and was equally sensitive to benzaldehyde and octanal. Likewise, glomeruli D and E, while both highly sensitive to benzaldehyde, showed strikingly different relative sensitivity profiles. Observations from single preparations are consistent with this result; the specificity of the receptor neuron populations innervating a glomerulus is often complex and not easily predicted from the chemical structure of a few effective odorants.

Concentration-response functions of input to glomeruli

We measured response amplitude versus odorant concentration for a variety of odorants, comparing different glomeruli in the same preparation, and well as comparing input to the same glomerulus evoked by different odorants. In total, concentration-response functions were measured for 28 glomeruli (12 preparations) tested with at least four concentrations over a range of at least 2 log units. Plotting response amplitude relative to resting fluorescence ($\Delta F/F$) as a function of concentration revealed that most (23/28) glomeruli showed continuous increases over this range, even at odorant dilutions as high as 11% of saturated vapor (5 - 430 μM vapor concentration). An example of this large dynamic range is shown for six glomeruli in Figures 6A and B. However, the

diffuse 'background' signal (spot b, Figure 6A), which presumably arises from out-of-focus and/or scattered light, also increased in amplitude with odorant concentration (Figure 6B). Thus, the continuous increase in glomerular signal amplitude might in part be due to increases in the background signal associated with increased signals in neighboring glomeruli. We therefore also measured response amplitude relative to the local background (see Methods), as done in intrinsic imaging studies (Rubin and Katz, 1999; Meister and Bonhoeffer, 2001). Figure 6C shows the same responses to 2-hexanone as in Figure 6B, measured relative to background, and shows an apparent saturation in the concentration-response functions of some glomeruli. Other glomeruli, however, continue to show increases in response amplitude over the entire concentration range. In total, 18 of the 28 concentration-response functions showed no sign of saturation after background correction. In the 10 glomeruli that did appear to saturate, the kinetics of the evoked response did not change at saturating concentrations (not shown), suggesting that this effect is not due to saturation of calcium binding to Calcium Green-1 dextran.

Figure 6C suggests that the dynamic range (and therefore the normalized activation slope) of input to a glomerulus can differ for different glomeruli. For example, glomeruli 3 and 4 appear to saturate above 9 μM hexanone, while glomeruli 5, 6, 2 and 1 do not. We estimated the slope of each of the 28 concentration-response functions (measured relative to background) by fitting to the following equation:

$$R = \frac{C^n}{C^n + k^n} . \qquad (1)$$

This form is equivalent to the Hill equation with R_{max} , the maximal response, set equal to 1, where R is the measured response amplitude, k is the half-saturating concentration and n (the Hill coefficient), is a measure of the slope. Each concentration-response function was normalized to its own maximum before fitting. Figure 6D shows a histogram of Hill coefficients for the 28 fits. The fitted slopes showed considerable variability, with n ranging from 0.5 to 1.9, supporting our observation that different glomeruli can have quite different concentration-response functions. For the 18 concentration-response functions that did not show saturation, the values for n are very likely overestimates. Despite this bias towards overestimation, the values were low compared to Hill coefficients reported for individual salamander olfactory receptor neurons (n = 1.9 - 4.4; Firestein et al., 1993).

We also measured concentration-response functions for the same glomerulus in response to different odorants. Figure 6E shows concentration-response plots for three glomeruli activated by 2-hexanone and 2-butanone. Each glomerulus is more sensitive to 2-hexanone than to 2-butanone, but the slopes and maximal responses amplitudes are similar. Figure 6F compares the fits of equation (1) to the concentration-response plots obtained for glomerulus 4 in response to 2-hexanone and 2-butanone. The fits yield similar n values, and both responses are well-fit using a single n (Figure 6F). Similar n values for responses to these two odorants were also obtained for glomeruli 3 and 6 (not shown).

In contrast to this result, we noticed that, for the identified glomerulus B (see Figures 4A, B, Figure 5), the structurally similar odorants hexyl acetate and isoamyl acetate showed quite distinct concentration-response functions (Figure 7A). This

glomerulus was consistently more sensitive to hexyl acetate than to isoamyl acetate, but the concentration-response function for isoamyl acetate was steeper. As shown in Figure 7B, the Hill coefficients determined from fitting the two responses to equation (1) were quite different. The kinetics of activation of glomerulus B for these two odorants did not differ. We compared the concentration-response functions of glomerulus B for these two odorants in three additional animals. In two of the three, the two responses were also poorly fit by a single slope value, with a steeper concentration-dependence for isoamyl acetate than for hexyl acetate (n, hexyl acetate = 0.6 ± 0.1 and 0.9 ± 0.2; n, isoamyl acetate = 1.1 ± 0.1 and 1.8 ± 0.6). In the fourth animal, the two slopes were equal (n = 1.8 ± 0.1 and 1.8 ± 0.7), although hexyl acetate was only tested over a small part of its dynamic range. Thus, in addition to differences in the concentration-response functions of receptor neuron input to different glomeruli, the concentration-dependence of input to the the same glomerulus can differ for different odorants.

Discussion

Distributed odorant representations

We used *in vivo* loading of olfactory receptor neurons with a calcium-sensitive dye to image odorant representations at the level of receptor neuron input to the mouse olfactory bulb. At near-threshold odorant concentrations, we observed a broad chemotopy in the distribution of receptor neuron input to the dorsal bulb that was organized according to functional group. Most glomeruli activated by aliphatic aldehydes and fatty acids were located anteromedially, while those activated by ketones and acetates were located caudal-laterally. These regions correspond approximately to the anteromedial and lateral domains identified in the rat using intrinsic imaging signals (Uchida et al. 2000). However, most odorants also evoked input to at least some glomeruli outside of these domains, implying that, at least in the mouse, the chemotopic projection of receptor neurons to olfactory bulb glomeruli is only loosely defined.

We observed that even moderate increases in odorant concentration recruited input to a large number of glomeruli, causing substantial changes in the odorant response maps. This result is consistent with previous reports of concentration-dependent recruitment of glomeruli (Rubin and Katz, 1999; Sachse et al., 1999; Johnson and Leon, 2000; Meister and Bonhoeffer, 2001), and recruitment of individual olfactory receptor neurons (Malnic et al., 1999; Ma and Shepherd, 2000). In contrast, however, maps of receptor neuron input to the turtle olfactory bulb vary little with concentration (Wachowiak et al. 2000a, b). Thus, the concentration-dependence of odorant representations may differ across species. In addition, studies using fMRI, 2-deoxyglucose, or c-*fos* imaging in rats have reported concentration-invariant maps of glomeruli activation for at least some odorants (Johnson and Leon, 2000; Xu et al., 2000; Schaefer et al. 2001), suggesting that the effect of concentration on pre- and post-synaptic odorant representations may also differ.

Surprisingly, recruited glomeruli were distributed widely across the dorsal bulb, and in areas well outside the regions reported to be activated by these odorants using intrinsic imaging or 2-deoxyglucose metabolism (Johnson and Leon, 2000; Uchida et al., 2000; Belluscio and Katz, 2001; Meister and Bonhoeffer, 2001). Significant recruitment

was seen for all odorants tested, with odorants often eliciting input to a substantial fraction of all glomeruli in the imaged region. The concentrations at which this recruitment was observed were moderate: the vapor dilutions (0.3 - 2%) and molar vapor concentrations (≤ 1 μM for most odorants) are comparable to or lower than those used in measuring odorant-evoked activation of single rodent olfactory receptor neurons (Bozza and Kauer, 1998; Duchamp-Viret et al., 2000; Ma and Shepherd, 2000; Malnic et al., 2000; Reisert and Matthews, 2001), or in previous imaging studies (Johnson and Leon, 2000; Uchida et al., 2000; Belluscio and Katz, 2001; Meister and Bonhoeffer, 2001). These concentrations were also well within the dynamic range of input to imaged glomeruli (see below), and were well within the range of concentrations over which rats and mice can perform odor discrimination and odor quality recognition tasks (Youngentob et al.,1990; Lu and Slotnick, 1998; Bodyak and Slotnick, 1999). We have observed a similar widespread distribution of receptor neuron input to the turtle olfactory bulb (Wachowiak et al., 2000a, b). Our results suggest that representations of even moderate concentrations of monomolecular odorants involve receptor neuron input to fairly large numbers of glomeruli distributed across much of the olfactory bulb.

Specificity of receptor neuron input to individual glomeruli

Five glomeruli were functionally identified across animals by locating individual glomeruli activated in the same location of the bulb in response to near-threshold concentrations of one or, occasionally, two 'search' odorants. These identified glomeruli were not always the glomeruli most sensitive to that odorant, nor were they the most strongly-activated at higher odorant concentrations - they were simply the most easily isolated. However, the ability to identify the same glomerulus in most animals allowed us, for the first time in a vertebrate, to compile information about the specificity and concentration-response functions of the same receptor neuron population across animals.

The relative sensitivity to a range of odorants was consistent across animals. We also found that the response specificity of all five glomeruli was complex and not easily predicted on the basis of odorant structure. Because receptor neurons expressing the same receptor protein converge onto the same glomerulus (Mombaerts et al., 1996), these results are consistent with earlier studies showing that many receptor proteins show complex odorant binding specificities. (Malnic et al., 1999; Ma and Shepherd, 2000; Duchamp-Viret et al., 2000). In contrast, a recent characterization of the rat I7 receptor reported a high selectivity for octanal and closely-related aldehydes (Araneda et al., 2000). Thus, different receptor proteins may exhibit different degrees of selectivity.

Concentration-response functions of input to olfactory bulb glomeruli

Our measurements indicate that the dynamic range of receptor neuron input to a glomerulus is large. The majority of tested glomeruli showed a dynamic range of at least 2 log units. In contrast, studies of individual amphibian and mammalian receptor neurons report dynamic ranges of 1 log unit or less (Firestein et al., 1993; Trotier et al., 1994; Reisert and Matthews, 2001). Likewise, fitting the concentration-response measurements to a form of the Hill equation which was biased towards overestimation of the Hill coefficient yielded a range of coefficients (n = 0.5 - 1.9) that were low relative to those reported for salamander olfactory receptor neurons (n = 1.9 - 4.4; Firestein et al., 1993).

Previous calcium imaging studies of receptor neuron input to glomeruli in the zebrafish and turtle have reported similarly large dynamic ranges (Friedrich and Korsching, 1997; Wachowiak et al., 2000a). This expanded dynamic range could be explained by different odorant sensitivities expressed across a population of convergent receptor neurons (Firestein et al., 1993; Cleland and Linster, 1999).

We also found that the slope of the concentration-response function could differ for different glomeruli. This result is in contrast to a recent intrinsic imaging study reporting that the concentration-response functions of all glomeruli have similar slopes (Meister and Bonhoeffer et al., 2001). In fact, we found that the concentration-response slope measured from the same glomerulus (and presumably the same receptor neuron population) could differ for different odorants. This result is surprising given that single olfactory receptor neurons show parallel concentration-response functions for different odorants (Firestein et al., 1993; Trotier, 1994). A possible explanation for this effect is that the two odorants have differential access to the same population of receptor neurons *in vivo*, for example due to differential sorption onto the olfactory epithelium (Kent et al., 1996). The different concentration-response functions might also reflect differential efficacy of these two ligands in receptor activation (e.g. - partial agonism; Jasper and Insel, 1992; Araneda et al. 2000).

Comparison with intrinsic signals from the olfactory bulb

A number of our observations differ significantly from those reported in recent intrinsic imaging studies. One is our finding that odorants evoke significant input to a larger number of more widely distributed glomeruli than reported previously. For example, Belluscio and Katz (2001) reported that aldehyde dilutions of 1 - 2% activated, on average, 4 – 6 glomeruli on the dorsal surface of the mouse olfactory bulb, while we observed an average of 22 ± 3 (n=10) glomeruli activated at the same concentrations. This difference may be explained by the increased signal-to-noise ratio of the calcium imaging method and by the thresholding of the response maps in the Belluscio and Katz (2001) study (see Figure 3C). However, high-pass filtering the calcium signal, as has been done in other intrinsic imaging studies (Meister and Bonhoeffer, 2001), did not reduce the number of apparent glomeruli, suggesting that the smaller number of glomeruli observed with intrinsic imaging cannot be accounted for simply by differences in processing of the optical signal.

There were also significant qualitative differences in patterns of glomerular activation observed in the present study and in intrinsic imaging studies. These differences include the specificity and distribution of glomeruli activated by particular odorants, and the concentration-response functions of individual glomeruli, as discussed above. While these differences might be partly explained by the lower signal-to-noise ratio of the intrinsic signal, they also likely reflect differences in the signal source. Indeed, preliminary pharmacological experiments suggest that the intrinsic signal primarily tracks postsynaptic activity (M. Meister, personal communication). In addition, our measurements reflect peak levels of presynaptic action potential firing during the first 100 - 400 ms after odorant stimulation, while the intrinsic signal measurements reflects activity integrated over ~ 10 seconds, a time over which odorant representations may be shaped substantially by synaptic processing. Thus, differences in specificity, distribution,

and concentration-response functions may reflect real differences in the representation of odorants at pre- vs. postsynaptic levels. Simultaneous imaging of presynaptic calcium and intrinsic signals will be important in addressing these issues.

Emergent features of odorant representations

Selectively labeling olfactory receptor neurons with a calcium-sensitive dye has allowed us to begin characterizing the odorant response properties of receptor neuron populations after their convergence onto individual glomeruli. Some of these properties, in particular the dynamic range and slopes of the concentration-response functions, differ from those reported for individual receptor neurons (Firestein et al., 1993; Trotier et al., 1994; Reisert and Matthews, 2001). Thus, the convergence of receptor neurons onto olfactory bulb glomeruli results in more than a simple transformation of a distributed receptor code into a spatially-organized glomerular code; it also appears to add new features to odorant representations that are not present at the single-neuron level. Emergent features at the level of input to olfactory bulb glomeruli might also result from presynaptic inhibition of transmitter release from receptor neurons (Wachowiak and Cohen, 1999; Hsia et al., 1999; Aroniadou-Anderjaska et al., 2000). Any effects of presynaptic inhibition on odorant representations should be reflected in the optical signals measured here. Given our evidence that glomeruli can be functionally identified across animals, it should be possible to investigate these features more extensively. For example, identified glomeruli can potentially be matched with their respective olfactory receptor genes, allowing a direct comparison of the response properties of neurons expressing a known olfactory receptor at the single-neuron and population levels.

Emergent features of glomerular odorant representations are also likely to arise from postsynaptic processing. By imaging activity from additional specified neuronal populations, the transformation of odorant representations by postsynaptic processing might be visualized directly. For example, imaging mitral/tufted cell activity with voltage- or calcium-sensitive dyes (e.g. - Charpak et al., 2000) would allow comparison of receptor neuron input maps with maps of olfactory bulb output. This general approach is likely to be useful in gaining a better understanding of how olfactory information is represented and processed at different levels of the mammalian olfactory pathway.

Experimental Procedures

Additional information regarding dye loading, optical recording and odorant presentation is provided as Supplemental Information, and can be accessed online at [link here].

Dye loading

Experiments were performed on 25 female and 5 male C57/Bl6 mice, 8 - 12 wks of age. Olfactory receptor neurons were loaded *in vivo* with Calcium Green-1 dextran, 10 kD m.w. (Molecular Probes, Eugene OR) using a protocol adapted from Friedrich and Korsching (1997). Mice were anesthetized with ketamine (90 mg/kg) and xylazine (10 mg/kg). 2 µl of 0.25% Triton-X 100 was injected into the nasal cavity. After 60 sec, 8 µl of 4% Calcium Green-1 dextran was injected at a rate of ~ 0.4 µl/min. Mice recovered from anesthesia and were held for 4 - 8 days before imaging.

Imaging

Mice were anesthetized with pentobarbital (50 mg/kg, i.p.), and atropine (5 mg/kg) was injected subcutaneously. A double tracheotomy was performed to allow control of odorant access to the nasal cavity. The mice breathed freely through the lower tracheotomy tube. Mice were secured in a stereotaxic headholder and the skin overlying the dorsal skull retracted. Local anesthetic (1% bipuvicaine) was applied to all incisions. The bone overlying the olfactory bulbs was thinned and ringers solution and a coverslip was placed over the exposed area. Body temperature was maintained at 37 C. Heart rate was maintained at 400 - 500 bpm by periodic injection of pentobarbital, and was additionally stabilized by directing a stream of pure oxygen over the lower tracheotomy tube. All procedures were approved by the Yale University and Marine Biological Laboratory animal care committees.

The dorsal surface of one olfactory bulb was illuminated with 480 ± 25 nm light using a 150W Xenon arc lamp (Opti-Quip, New York) and 515 nm long-pass dichroic mirror, and fluorescence emission above 530 nm was collected. Images were acquired and digitized with a 80 x 80 pixel CCD camera (NeuroCCD; RedShirtImaging LLC, Fairfield, CT) at 100 - 200 Hz and time-binned to a 25 Hz frame rate before storing to disk. Fluorescence was imaged using a 10.5x, 0.2 n.a. objective (spatial resolution, 22 μm per pixel assuming no scattering or out-of-focus signals) or a 14x, 0.4 n.a. objective (16.5 μm per pixel resolution).

Odorant presentation.

Odorants were obtained from Sigma or Fluka (all >99% pure). Odorants were diluted from saturated vapor with cleaned, dessicated air using a flow dilution olfactometer described previously (Lam et al., 2000). Odorant concentrations are reported as percent dilution from saturated vapor and as molar vapor concentrations. Vapor concentrations were calculated using the vapor pressure equation and appropriate coefficients, both provided by Yaws (1994). The accuracy and stability of the flow dilution system over the range used was confirmed with a photoionization detector. Dedicated lines for each odorant avoided cross-contamination.

An artificial sniff paradigm controlled odorant access to the nasal cavity. Square pulses of negative pressure (100 ml/min flow rate, 150 ms duration, 3.3 Hz) were applied to the upper tracheotomy tube. Sniffing was maintained throughout the experiment, with brief rest periods every several minutes. Cleaned, humidified air was continuously blown over the nares to prevent drying and was switched off during odorant presentation. The olfactometer delivered square-shaped, 1 sec duration odorant pulses at a flow rate of 300 ml/min. We waited a minimum of 60 sec between trials. Repeated presentations of the same odorant at this interstimulus interval evoked similar-amplitude signals.

Data processing and analysis.

While odorant-evoked signals were detected in single trials (see Figure 1), we typically collected, then averaged, responses of two to eight consecutive odorant presentations in order to improve the signal-to-noise ratio and to obtain a measure of trial-to-trial variability. All trials were saved to disk and inspected for consistency before

averaging. The signal amplitudes from consecutive, repeated odorant presentations typically varied by less than 10% (Figures 1F and 7A). Responses to repeated odorant presentations showed no sign of the Cohen Effect (Wachowiak and Cohen, 1999). The primary source of extrinsic noise was movement associated with respiration and heartbeat. The noise was largest in regions adjacent to major blood vessels, and so pixels overlying these regions were removed from the dataset (omitted) prior to analysis. Pixels receiving light from areas outside of the bulb were also omitted. Occasional trials with widespread artifactual signals (primarily due to movement) were discarded before averaging. After averaging, data from each pixel were temporally filtered with a 1 Hz low-pass Gaussian and a 0.017 Hz high-pass digital RC filter (both filters have a low sharpness). To partially correct for unequal labeling of glomeruli, the signal from each pixel was divided by its resting fluorescence obtained at the beginning of each trial. While we observed that the rise-time of the odorant-evoked signal could vary by as much as 200 ms in different glomeruli and for different odorants (not shown), in the present study we focused only on the spatial maps of receptor neuron input. To construct the maps, response amplitudes for each pixel were measured by subtracting the temporal average of a 400 ms time window just preceding the stimulus from a 400 ms temporal average centered around the peak of the response. The time windows were the same for all pixels in a given trial. For display, the map of response amplitudes was smoothed slightly by increasing the pixel dimensions from 80 x 80 to 160 x 160 and interpolating between pixels. Response maps were normalized to the maximum signal amplitude for that trial. Except in Figures 3B and C, no spatial filtering or background subtraction was performed.

Response amplitudes for individual glomeruli were measured from the maps in two ways: by averaging responses from 4 adjacent pixels in the center of the glomerulus, and by measuring the amplitude of a one-dimensional Gaussian function fit to a profile (2 - 4 pixels wide) of the signal through a glomerulus (Meister and Bohoeffer 2001). The first method gives a measure of signal amplitude relative to the resting fluorescence, while the second method gives a measure of amplitude relative to the local background signal.

Strongly-activated glomeruli were easily counted by visual inspection. For counting glomeruli with smaller-amplitude signals, the signal profile was fit to a gaussian and evaluated according to criteria for size (half-width within 2 s.d. of the mean measured for 101 test glomeruli (see Results)), amplitude (amplitude > 5 times the rms spatial noise, measured from adjacent non-activated areas), and appearance in multiple trials. Signals from out-of-focus regions of the preparation were not included in counts of glomeruli.

Concentration-response functions were normalized and fit to equation (1) using the Levenberg-Marquardt algorithm. All other data processing and display was performed with NeuroCCD software and with custom software written in IDL and LabVIEW.

Acknowledgments

We thank B. Ache, M. Djurisic, C. Greer, G. Shepherd, A. Yamaguchi, M. Zochowski and D. Zecevic for helpful comments on the manuscript. We also

thank Jessica Hanover and Michael Stryker for demonstrating their *in vivo* mouse preparation, C.-X.. Falk for continued improvements to the data acquisition and analysis software, and B. Lipscomb for generating the confocal olfactory bulb image. This work was supported by NIH NS08437-DC05259 and DC00378-03.

References

Adamek, G. D., Gesteland, R. C., Mair, R. G., and Oakley, B. (1984) Transduction physiology of olfactory receptor cilia. Brain Res, 310: 87-97.

Adrian, E. D. (1953) Sensory messages and sensation. The response of the olfactory organ to different smells. Acta Physiol Scand, 29: 5-14.

Aroniadou-Anderjaska, V., Zhou, F.-M., Priest, C. A., Ennis, M., and Shipley, M. T. (2000) Tonic and synaptically evoked presynaptic inhibition of sensory input to rat olfactory bulb via $GABA_B$ heteroreceptors. J Neurophysiol, 84: 1194-1203.

Belluscio, L., and Katz, L. C. (2001) Symmetry, stereotypy, and topography of odorant representations in mouse olfactory bulbs. J Neurosci, 21: 2113-2122.

Bodyak, N., and Slotnick, B. (1999) Performance of mice in an automated olfactometer: Odor detection, discrimination and odor memory. Chem Senses, 24: 637-645.

Bozza, T. C., and Kauer, J. S. (1998) Odorant response properties of convergent olfactory receptor neurons. J Neurosci, 18: 4560-4569.

Charpak, S., Mertz, J., Beaurepaire, E., Moreaux, L., and Delaney, K. (2000) Odor-evoked calcium signals in dendrites of rat mitral cells. Proc Natl Acad Sci USA, 98: 1230-1234.

Cleland, T. A., and Linster, C. (1999) Concentration tuning mediated by spare receptor capacity in olfactory sensory neurons: A theoretical study. Neural Computation, 11: 1673-1690.

Duchamp-Viret, P., Duchamp, A., and Chaput, M. A. (2000) Peripheral odor coding in the rat and frog: quality and intensity specification. J Neurosci, 20: 2383-2390.

Fetcho, J. R., and O'Malley, D. M. (1995) Visualization of active neural circuitry in the spinal cord of intact zebrafish. J Neurophysiol, 73: 399-406.

Firestein, S., Picco, C., and Menini, A. (1993) The relation between stimulus and response in olfactory receptor cells of the tiger salamander. J Physiol, 468: 1-10.

Friedrich, R. W., and Korsching, S. I. (1998) Chemotopic, combinatorial and noncombinatorial odorant representations in the olfactory bulb revealed using a voltage-sensitive axon tracer. J Neurosci, 18: 9977-9988.

Friedrich, R. W., and Korsching, S. I. (1997) Combinatorial and chemotopic odorant coding in the zebrafish olfactory bulb visualized by optical imaging. Neuron, 18: 737-752.

Guthrie, K. M., Anderson, A. J., Leon, M., and Gall, C. (1993) Odor-induced increases in c-fos mRNA epression reveal an anatomical "unit" for odor processing in the olfactory bulb. Proc Natl Acad Sci USA, 90: 3329-3333.

Hsia, A. Y., Vincent, J.-D., and Lledo, P.-M. (1999) Dopamine depresses synaptic inputs into the olfactory bulb. J Neurophysiol, 82: 1082-1085.

Jasper, J. R., and Insel, P. A. (1992) Evolving concepts of partial agonism. The beta-adrenergic receptor as a paradigm. Biochem Pharmacol, 43: 119-130.

Johnson, B. A., and Leon, M. (2000) Modular representations of odorants in the glomerular layer of the rat olfactory bulb and the effects of stimulus concentration. J Comp Neurol, 422: 496-509.

Johnson, B. A., Woo, C. C., and Leon, M. (1998) Spatial coding of odorant features in the glomerular layer of the rat olfactory bulb. J Comp Neurol, 393: 457-471.

Kauer, J. S. (1991) Contributions of topography and parallel processing to odor coding in the vertebrate olfactory pathway. Trends Neurosci, 14: 79-85.

Kent, P. F., Mozell, M. M., Murphy, S. J., and Hornung, D. E. (1996) The interaction of imposed and inherent olfactory mucosal activity patterns and their composite representation in a mammalian species using voltage-sensitive dyes. J Neurosci, 16: 345-353.

Kreitzer, A. C., Gee, K. R., Archer, E. A., and Regehr, W. G. (2000) Monitoring presynaptic calcium dynamics in projection fibers by in vivo loading of a novel calcium indicator. Neuron, 27: 25-32.

Lam, Y.-W., Cohen, L. B., Wachowiak, M., and Zochowski, M. R. (2000) Odors elicit three different oscillations in the turtle olfactory bulb. J Neurosci, 20: 749-762.

LaMantia, A.-S., Pomeroy, S. L., and Purves, D. (1992) Vital imaging of glomeruli in the mouse olfactory bulb. J Neurosci, 12: 976-988.

Lu, X.-C. M., and Slotnick, B. M. (1998) Olfaction in rats with extensive lesions of the olfactory bulbs: implications for odor coding. Neuroscience, 84: 849-866.

Ma, M., and Shepherd, G. M. (2000) Functional mosaic organization of mouse olfactory receptor neurons. Proc. Natl. Acad. Sci. USA, 23: 12869-12874.

Malnic, B., Hirono, J., Sato, T., and Buck, L. B. (1999) Combinatorial receptor codes for odors. Cell, 96: 713-723.

Meister, M., and Bonhoeffer, T. (2000) Tuning and topography in an odor map on the rat olfactory bulb. J Neurosci, 21: 1351-1360.

Mombaerts, P., Wang, F., Dulac, C., Chao, S., Nemes, A., Mendelsohn, M., Edmondson, J., and Axel, R. (1996) Visualizing an olfactory sensory map. Cell, 87: 597-609.

O'Connell, R. J., and Mozell, M. M. (1969) Quantitative stimulation of frog olfactory receptors. J Neurophysiol, 32: 51-63.

O'Donovan, M. J., Ho, S., Sholomenko, G., and Yee, W. (1993) Real-time imaging of neurons retrogradely labeled with calcium sensitive dyes. J Neurosci Meth, 46: 91-106.

Rawson, N. E., Eberwine, J., Dotson, R., Jackson, J., Ulrich, P., and Rostrepo, D. (2000) Expression of mRNAs encoding for two different olfactory receptors in a subset of olfactory receptor neurons. J Neurochem, 75: 185-195.

Reisert, J., and Matthews, H. (2001) Response properties of isolated mouse olfactory receptor cells. J Physiol, 530: 113-122.

Ressler, K. J., Sullivan, S. L., and Buck, L. B. (1994) Information coding in the olfactory system: evidence for a stereotyped and highly organized map in the olfactory bulb. Cell, 79: 1245-1255.

Rubin, B. D., and Katz, L. C. (1999) Optical imaging of odorant representations in the mammalian olfactory bulb. Neuron, 23: 499-511.

Sachse, S., Rappert, A., and Galizia, C. G. (1999) The spatial representation of chemical structures in the antennal lobe of honeybees: steps toward the olfactory code. Eur J Neurosci, 11: 3970-3982.

Schaefer, M. L., Young, D. A., and Rostrepo, D. (2001) Olfactory fingerprints for major histocompatibility complex-determined body odors. J Neurosci, 21: 2481-2487.

Shepherd, G. M. (1994) Discrimination of molecular signals by the olfactory receptor neuron. Neuron, 13: 771-790.

Stewart, W. B., Kauer, J. S., and Shepherd, G. M. (1979) Functional organization of rat olfactory bulb analysed by the 2-deoxyglucose method. J Comp Neurol, 185: 715-734.

Strotmann, J., Conzelmann, S., Beck, A., Feinstein, P., Breer, H., and Mombaerts, P. (2000) Local permutations in the glomerular array of the mouse olfactory bulb. J Neurosci, 20: 6987-6938.

Trotier, D. (1994) Intensity coding in olfactory receptor cells. Sem Cell Biol, 5: 47-54.

Tsau, Y., Wenner, P., O'Donovan, M. J., Cohen, L. B., Loew, L. M., and Wuskell, J. P. (1996) Dye screening and signal-to-noise ratio for retrogradely transported voltage-sensitive dyes. J Neurosci Methods, 70: 121-9.

Uchida, N., Takahashi, Y. K., Tanifuji, M., and Mori, K. (2000) Odor maps in the mammalian olfactory bulb: domain organization and odorant structural features. Nat Neurosci, 3: 1035-1043.

Vassar, R., Chao, S. K., Sitcheran, R., Nunez, J. M., Vosshall, L. B., and Axel, R. (1994) Topographic organization of sensory projections to the olfactory bulb. Cell, 79: 981-991.

Wachowiak, M., and Cohen, L. B. (1999) Presynaptic inhibition of primary olfactory afferents mediated by different mechanisms in lobster and turtle. J Neurosci, 19: 8808-8817.

Wachowiak, M., Cohen, L. B., and Zochowski, M. (2000) Spatial patterns of olfactory receptor neuron input to turtle olfactory bulb glomeruli imaged with calcium-sensitive dyes. Chem Senses, 25: 675-675.

Xu, F., Kida, I., Hyder, F., and Shulman, R. G. (2000) Assessment and discrimination of odor stimuli in rat olfactory bulb by dynamic functional MRI. Proc. Natl. Acad. Sci. USA, 97: 10601-10606.

Yaws, C. (1994). Handbook of Vapor Pressures (Houston, TX: Gulf Publishing).

Yokoi, M., Mori, K., and Nakanishi, S. (1995) Refinement of odor molecule tuning by dendrodendritic synaptic inhibition in the olfactory bulb. Proc. Natl. Acad. Sci. USA, 92: 3371-3375.

Youngentob, S. L., Markert, L. M., Mozell, M. M., and Hornung, D. E. (1990) A method for establishing a five odorant identification confusion matrix task in rats. Physiol Behav, 47: 1053-1059.

Figure Legends

Figure 1. Imaging mouse olfactory receptor neuron activation after *in vivo* loading with Calcium Green dextran.

(A) Confocal image of a section through one olfactory bulb fixed 5 days after loading. Fixable rhodamine dextran (10 kD) was used instead of Calcium Green dextran to preserve labeling in fixed tissue. Glomeruli are strongly labeled. There is no evidence of transynaptic labeling. *onl*, olfactory nerve layer; *gl*, glomerular layer; *epl*, external plexiform layer.
(B) Resting Calcium Green dextran fluorescence imaged *in vivo*, 7 days after loading. The image was contrast-enhanced to emphasize individual glomeruli. Blood vessels appear as dark lines. The saturated regions in the upper right are from olfactory nerve bundles that obscure underlying glomeruli. Lines originate from two glomeruli whose responses are shown in (C) and (D).
(C) Hexanal evoked rapid (~200 ms rise-time) increases in fluorescence in the two glomeruli indicated in (B) (lines). Each trace shows the optical signal measured from one pixel and from a single trial. The dark traces are filtered from 0.017 - 2 Hz. The gray trace shows the same signal from the upper glomerulus without low-pass filtering. In this case (but not in most cases), small responses to individual sniffs (arrows) could be seen riding on the sustained fluorescence increase. Stimulation with clean air elicited no response (lower trace).
(D) Gray-scale map of the evoked signal for the trial shown in (C), showing foci of fluorescence increases. A region of the map normalized to 50% of the maximum signal (inset) shows additional smaller-amplitude foci. Signal foci in the upper portions of the image are blurred due to out-of-focus glomeruli and light scattering from overlying axons.
(E) Consecutive presentations of hexyl acetate in the same preparation evoked nearly identical responses. Each map is from a single trial. Note that the map evoked by hexyl acetate is different from that evoked by hexanal.
(F) Overlaid traces of responses from one glomerulus to the two presentations of hexyl acetate. Each trace is the spatial average of the same four pixels. The amplitude and time-course of the response was nearly identical in the two trials.

Figure 2. Responses to near-threshold odorant concentrations reveal a broad chemotopy of glomerular input.

(A) Response maps evoked by near-threshold concentrations of hexanal, 2-hexanone and hexyl acetate in one preparation. Hexanal activates four anteromedial glomeruli, while 2-hexanone and hexyl acetate activate several caudal-lateral glomeruli. Imaged region of the bulb is outlined in black. *n* indicates the number of trials averaged for each response map.
(B) Summary figure showing the location of glomeruli activated by the C6 aldehyde hexanal (red), C5 or C6 fatty acids (yellow), C4 or C6 ketones (green), the C6 ester hexyl acetate (blue) and the benzene derivative benzaldehyde (cyan), compiled from 12 preparations. Locations of glomeruli were aligned and plotted relative to the intersection

of the midline and the caudal sinus, as indicated by the x and y axes. For reference, the background shows the resting fluorescence of an imaged bulb.
(C) Response maps evoked by near-threshold concentrations of three aldehydes - propanal (C3), hexanal (C6) and octanal (C8), and the fatty acid hexanoic acid (C6). Several glomeruli, marked by arrows, are activated by all three odorants.While octanal activates several posterior glomeruli not strongly activated by the other aldehydes, there is no clear progression in the location of activated glomeruli with carbon chain length.

Figure 3. Increasing odorant concentration recruits input to many widespread glomeruli.

(A) Response maps evoked by a near-threshold (left) and a 15-fold higher concentration (right) of hexanal (14x magnification). The higher concentration evokes input to many more glomeruli. The maximal response amplitude (max $\Delta F/F$) also increases by a factor of 2.4.
(B) The same data as in part (A), left, after smoothing with a Gaussian kernel of width σ = 140 μm and subtracting the smoothed from the original image.
(C) The same data as in part (A), left, after thresholding at two SD above the mean.
(D) Summary images showing the locations of glomeruli activated by moderate concentrations (1 - 2% dilution of saturated vapor) of hexanal (red), hexyl acetate (blue), C4 or C6 ketones (green), and benzaldehyde (cyan). Glomerulus locations are aligned as described in Figure 2B. *n*, number of preparations for each odorant class. These data are mostly from the same preparations as in Figure 2B.
(E) Responses to 2-hexanone over a 165-fold concentration range (14x magnification). Different preparation than in (A). The number of apparent glomeruli increases more than three-fold, and the maximal response amplitude increases nearly ten-fold. Arrows point to two glomeruli that are recruited between 0.07% and 0.25% dilution.
(F) Response of the same preparation to 11% 2-butanone. 2-butanone activates many of the same glomeruli as 2-hexanone, but does not activate the two glomeruli recruited by 0.25% 2-hexanone (arrows).

Figure 4. Individual glomeruli can be functionally identified across animals.

(A) Pseudocolor maps showing the locations of five glomeruli (A through E) identified in multiple animals based on location and sensitivity to low concentrations of a 'search' odorant. Examples from two preparations are shown for each glomerulus. The overall identification rates for each glomerulus were: A, 23/34; B, 20/23; C, 6/20; D, 7/11; E, 12/12. For each map, the top 50% of the signal is superimposed on an image of the resting fluorescence. The horizontal and vertical dashed lines indicate the approximate medial-lateral and anterior-posterior meridians, respectively, of the bulb.
(B) Summary image showing the locations of glomeruli A through E from multiple preparations in which their location was determined relative to the midline and caudal sinus landmarks. Numbers indicate the number of preparations for each glomerulus.
(C) Response of glomerulus A to four odorants, measured in five preparations. In each, glomerulus A was activated by hexanal and hexanoic acid, and was insensitive to hexyl acetate and 2-hexanone. The diameter of each filled circle is proportional to the response

amplitude, relative to the response to hexanal. Open circles indicate no response. The numbers below each circle indicate the odorant dilution.

Figure 5. All five identified glomeruli show complex response specificities

Relative sensitivities of the glomeruli identified in Figure 4 to sixteen odorants, compiled across animals. Circles indicate the sensitivity of a glomerulus to an odorant, relative to its sensitivity to the primary odorant. The primary odorant was hexanal for glomerulus A, hexyl acetate for glomeruli B and C, and benzaldehyde for glomeruli D and E. The numbers below each circle indicate the number of preparations tested for each odorant; blank space indicates not tested. Concentrations indicate the mean vapor concentration of the primary odorant used in determining relative sensitivity (all concentrations were below 1 μM). Each glomerulus was sensitive to at least two odorants with different functional groups. Calculating relative sensitivity based on dilution of saturated vapor gave slightly different resur g response specificitied foraAll fivr g-1035(l)1.94(omerul.d)]TJ0 -2.36 TD-0.0005 Tc0.0005 Tw[(F)5.7(i)-2.7(g)9.5(u)-0.5(re6t. Thedty)29.5nar l omerul.d

A) Rresponse to2-(hex)-18(a-284none( )5. d)]TJ/TT3 1 Tf13.84 0 TD0 Tc0 Tw<021d>Tj/TT4 1 Tf0.54 0 TD-0

amplitud wasmleaur(e, relative to basline(fluo rencecse.A(bckng)8(r)7(uand s g)6nu)1(a (b) war)]TJT-0.00

to the value determined for the hexanone fit (in this case, n = 1.0). The colored text shows the n value for each fit, ± s.e.. The two responses are well-fit using the same n value.

Figure 7. The identified glomerulus B shows different activation slopes for different odorants.
(A) Concentration-response plots measured from glomerulus B in response to hexyl acetate (red, circles) and isoamyl acetate (blue, squares). Error bars indicate s.e.m. for the individual trials contributing to each data point (number of trials = 2 for the highest concentration, 4 for all other concentrations). The slope of the concentration-response plot is steeper for isoamyl acetate than for hexyl acetate.
(B) Comparison of the fits of the plots shown in (A) to equation (1). Red curve, fit to isoamyl acetate response. Green curve, fit to hexyl acetate response. Gray curve, fit to hexyl acetate response using n = 1.6 (determined from isoamyl acetate fit). The two responses are poorly fit using the same n value.

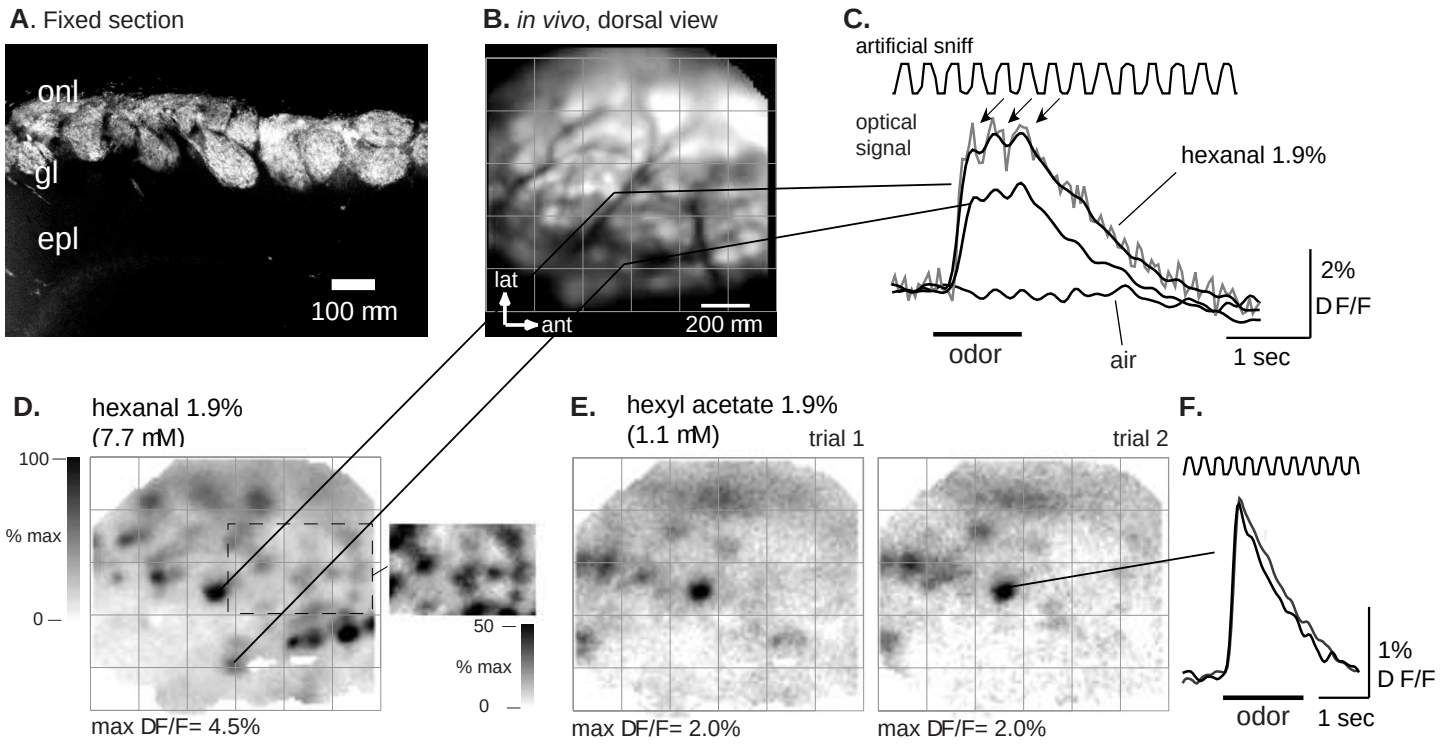

Figure 1
Wachowiak and Cohen

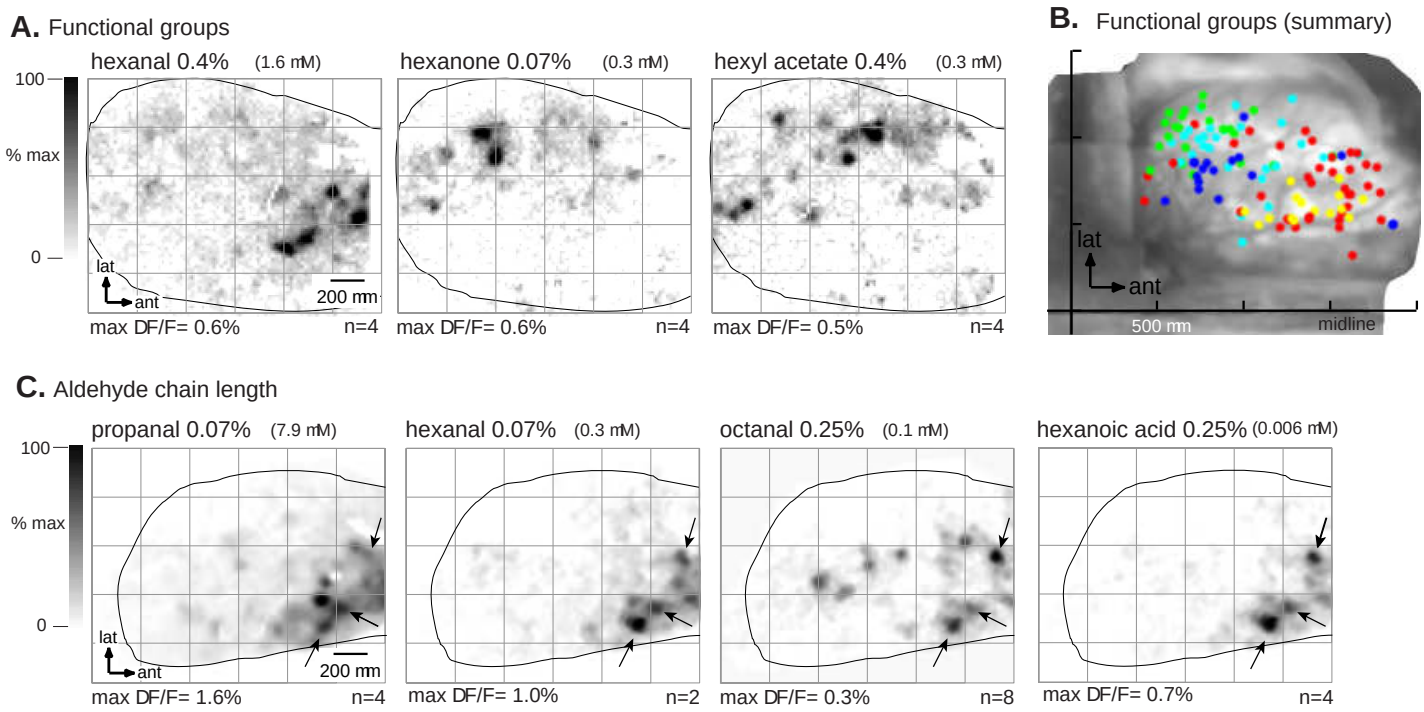

Figure 2
Wachowiak and Cohen

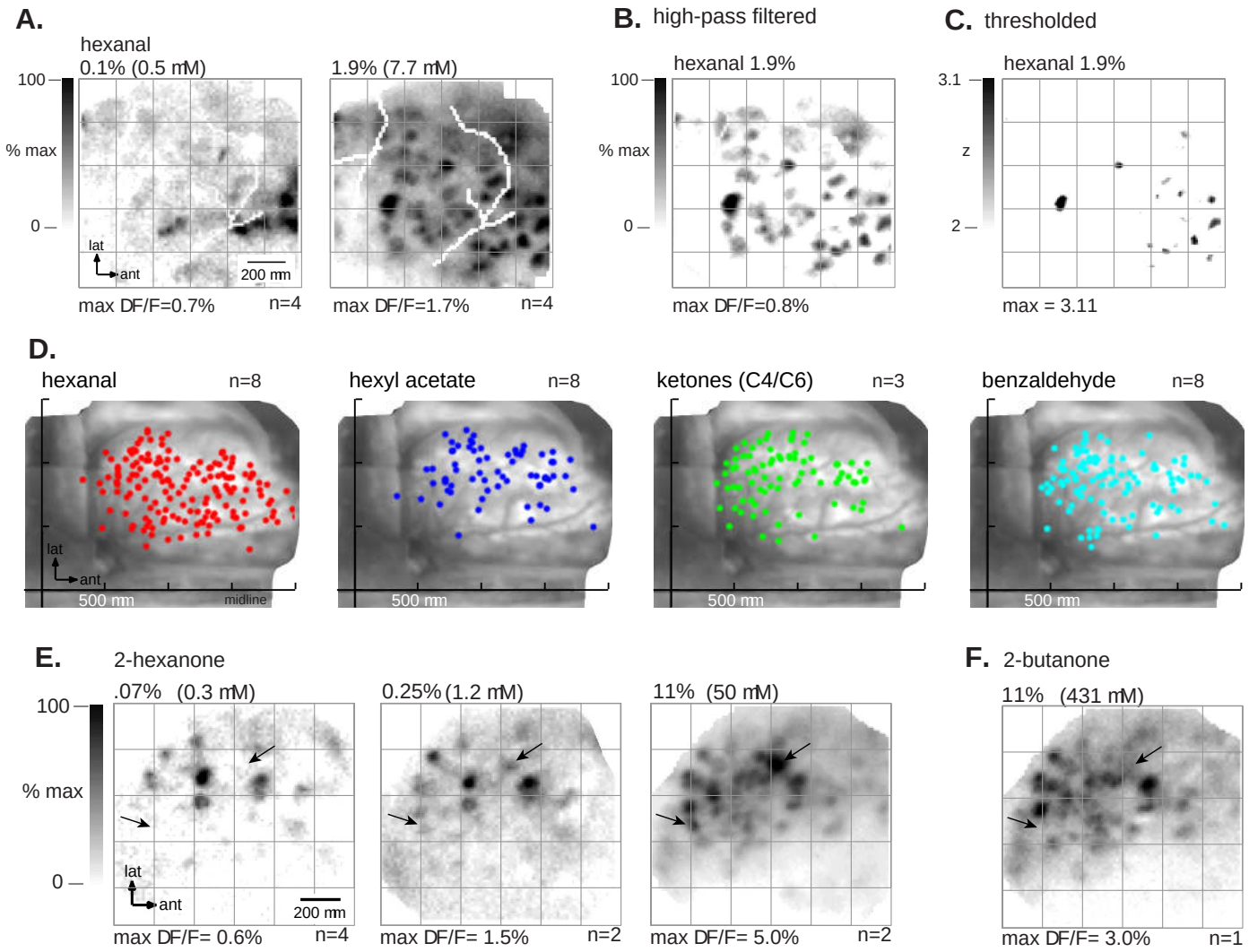

Figure 3
Wachowiak and Cohen

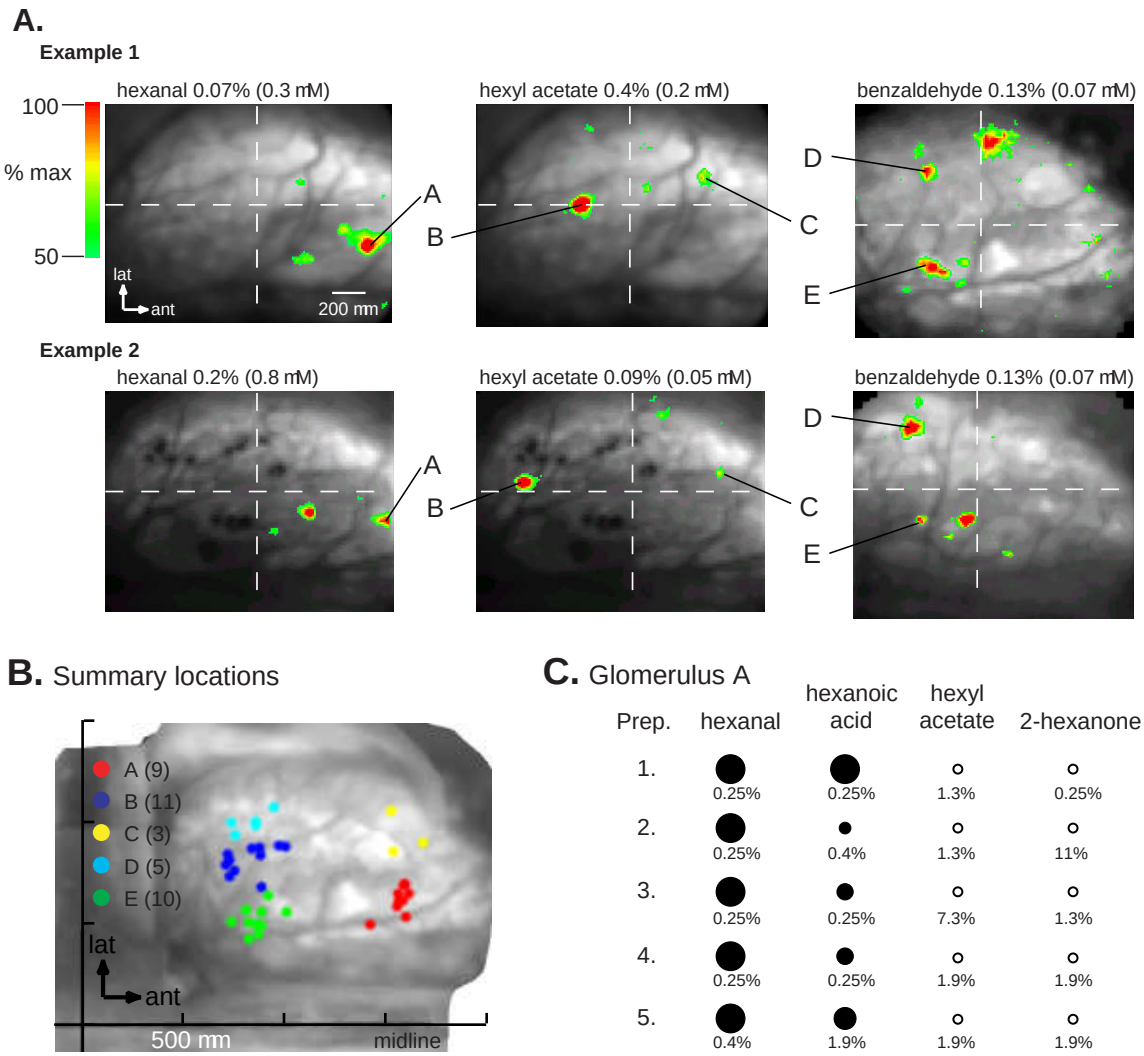

B. Summary locations

C. Glomerulus A

Prep.	hexanal	hexanoic acid	hexyl acetate	2-hexanone
1.	0.25%	0.25%	1.3%	0.25%
2.	0.25%	0.4%	1.3%	11%
3.	0.25%	0.25%	7.3%	1.3%
4.	0.25%	0.25%	1.9%	1.9%
5.	0.4%	1.9%	1.9%	1.9%

Figure 4
Wachowiak and Cohen

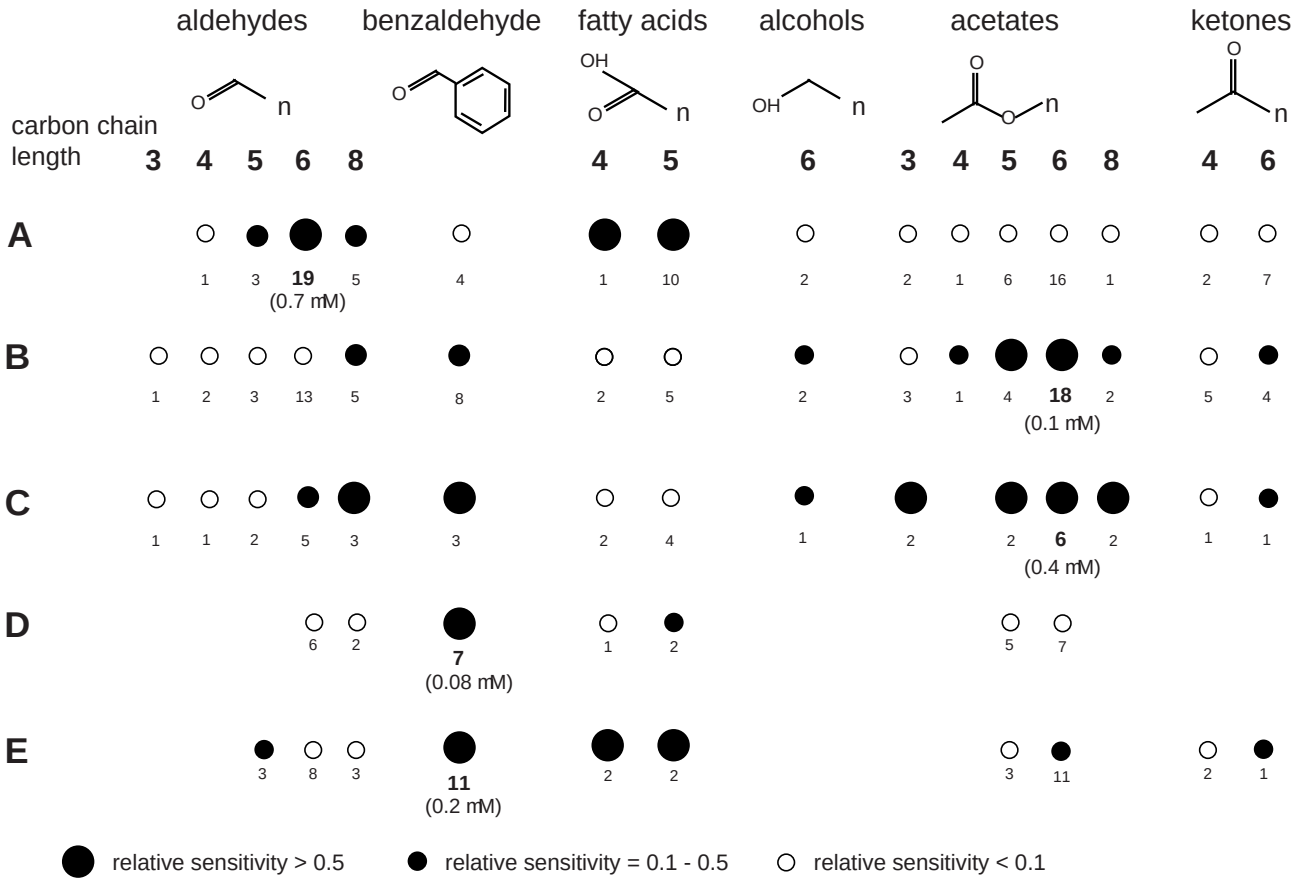

Figure 5
Wachowiak and Cohen

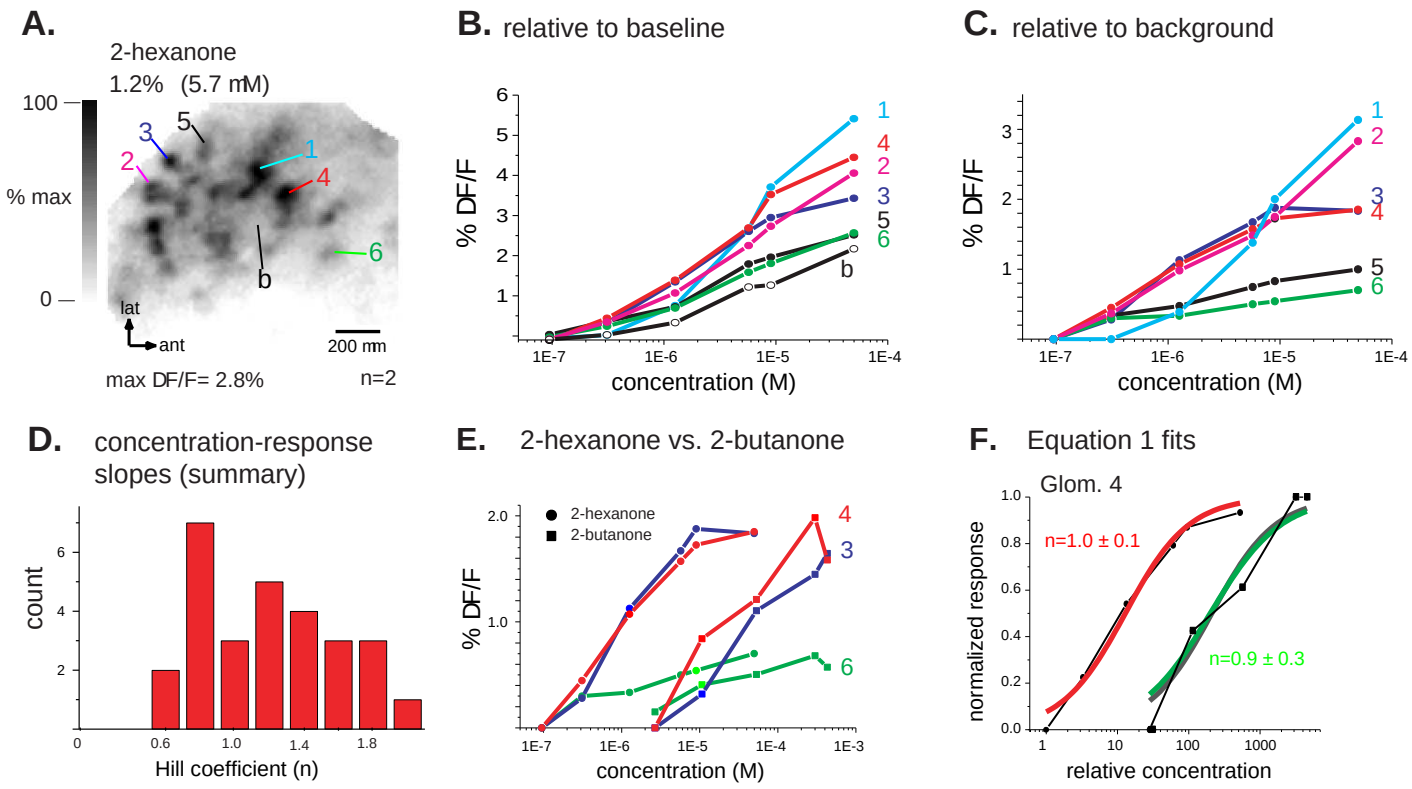

Figure 6
Wachowiak and Cohen

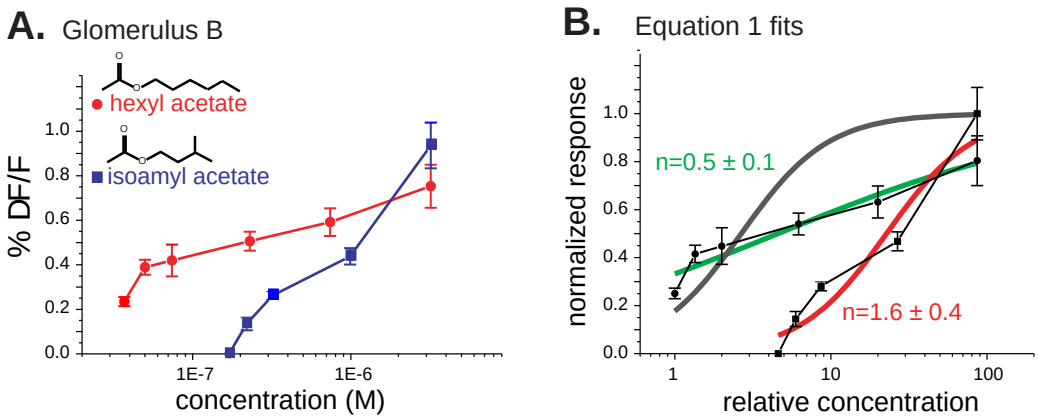

Figure 7
Wachowiak and Cohen

Supplemental Information

The following paragraphs contain additional information about procedures for loading olfactory receptor neurons with calcium-sensitive dyes and imaging calcium signals in the olfactory bulb. Included is information about alternative procedures that were tried and were less effective than those used in the present study.

Dye loading

Injection of Triton-X 100 and Calcium Green-1 dextran was performed using a homemade cannula and syringe pump. The cannula tip was constructed from pulled syringe tubing and was ~ 7 mm in length, which was sufficient to reach the back of the nasal cavity. Injection of a methylene blue solution and subsequent inspection of ORN staining in the epithelium was helpful in determining the position and length of insertion of the cannula for optimal loading. It was difficult to achieve homogeneous loading of olfactory receptor neurons projecting to glomeruli in all regions of the olfactory bulb. However, if the animal was placed on its back throughout the loading procedure, widespread labeling of most, if not all, dorsal glomeruli was achieved with a success rate of ~ 70%.

Several loading methods were evaluated for the most effective labeling of olfactory bulb glomeruli with minimal damage to the olfactory epithelium. A brief 'shock' of 0.25% Triton-X 100, followed by a slow wash with Calcium Green-1 dextran, was most effective. Application of Calcium Green-1 dextran in a solution of 0.05% Triton-X 100 for 20 min was also effective at loading receptor neurons but caused more damage to the epithelium. Higher detergent concentrations resulted in near total loss of the epithelium. Occasionally, axon terminals in olfactory bulb glomeruli were well-labeled but the epithelium was severely damaged, as evaluated by the lack of an EOG response or by visual inspection.

We found that injection of 4% Calcium Green-1 dextran (10 kD or 3kD m.w.) resulted in sufficiently bright labeling of olfactory bulb glomeruli. Concentrations of 2% or lower were considerably less bright. Calcium Green-1 dextran solution was stored at 4 C for up to 2 weeks before use. Freeze-thawing this solution appeared to result in loading of receptor neurons but little or no transport of dye to the axon terminal. Loading with Calcium Green-1 (not conjugated to dextran) also resulted in no transport. In several animals we loaded olfactory receptor neurons with 4% Fluo-4 dextran (Molecular Probes; Kreitzer et al., 2000). While loading and transport appeared to be successful with Fluo-4 dextran, labeling of glomeruli was less clear, presumably because of the low resting fluorescence of this probe (Kreitzer et al., 2000). Also, odorant-evoked Fluo-4 dextran signals were smaller in amplitude and not as reliably detected across preparations.

Imaging

In addition to the rapid, dye-dependent increase in fluorescence due to presynaptic calcium influx, odorants sometimes evoked a slower and longer-lasting decrease in

fluorescence, which we attributed to changes in the intrinsic optical properties of the olfactory bulb tissue (absorption or light scattering). This intrinsic signal was often only apparent at higher odorant concentrations (>1% of saturated vapor) and was strongest along major blood vessels (Figure 1). Focal signals indicative of glomeruli were not apparent with this intrinsic signal. In freely-breathing animals anesthetized with Nembutal, this signal had a slow onset and relatively small amplitude and so did not affect the spatial character or amplitude of the calcium signal. However, artificial respiration with pure oxygen caused an increase in the amplitude and speed of onset of the intrinsic signal such that the calcium signal was partially or completely obscured. A similar effect was seen in animals anesthetized with Urethane (3 g/kg, i.p.). We did not test other anesthetics.

Odorant presentation

We presented odorants using an artificial sniff paradigm and a double-barrel olfactometer that allowed for delivery of nearly square odorant pulses (Lam et al., 2000). This arrangement resulted in a more rapid onset in the odorant-evoked signal than in freely-breathing, Nembutal-anesthetized mice, which breathe at ~ 1 Hz (artificial sniffing was maintained at 3.3 Hz). The rapid signal onset was important in detecting small signals and in avoiding any effects of the intrinsic decrease in fluorescence (described above). The precise and rapid onset of the odorant and its evoked signal was also important in avoiding temporal smearing of responses averaged over multiple trials. The double tracheotomy also allowed us to stabilize the heartbeat with supplemental oxygen. In freely-breathing animals receiving supplemental oxygen directed at the nose, odorant presentation often caused slight changes in the level of inhaled oxygen, resulting in a large intrinsic optical signal that obscured the odorant-evoked calcium signal.

Figure 1 legend

Figure 1. Odorant stimulation can evoke decreases in fluorescence reflecting changes in intrinsic optical signals.
(A) Resting Calcium Green dextran fluorescence imaged from the dorsal olfactory bulb at 14x magnification. This image was not contrast-enhanced. This preparation was anesthetized with Nembutal and artificially ventilated with pure oxygen.
(B) Response map of the fluorescence increase evoked by hexanal. The map was constructed as described in the Experimental Methods, with the time-window for measuring response amplitude centered at t_1 (880 ms after odorant onset). In this map, lighter shades represent larger increases in fluorescence, with black indicating no change. There were no decreases in fluorescence apparent at this latency. Hexanal evokes input to many widespread glomeruli.. The time-course of the response measured from the two glomeruli indicated by the lines is shown in (D).
(C) Response map of the fluorescence decrease evoked by the same presentation of hexanal. The time-window for measuring response amplitude wascentered at t_2 (4000 ms after odorant onset). In this map, lighter shades represent larger decreases in fluorescence, with black indicating no change. There were no increases in fluorescence apparent at this latency. The largest decreases in fluorescence occur along blood vessels.
(D) Time-course of the optical signal recorded from the two locations indicated by the lines in (B) and (C). Each trace is from a single pixel and is filtered from 0.017 - 1 Hz. The top trace, which is from a location near a major blood vessel, shows a strong decrease in fluorescence (t_2) following the initial fluorescence increase (t_1).

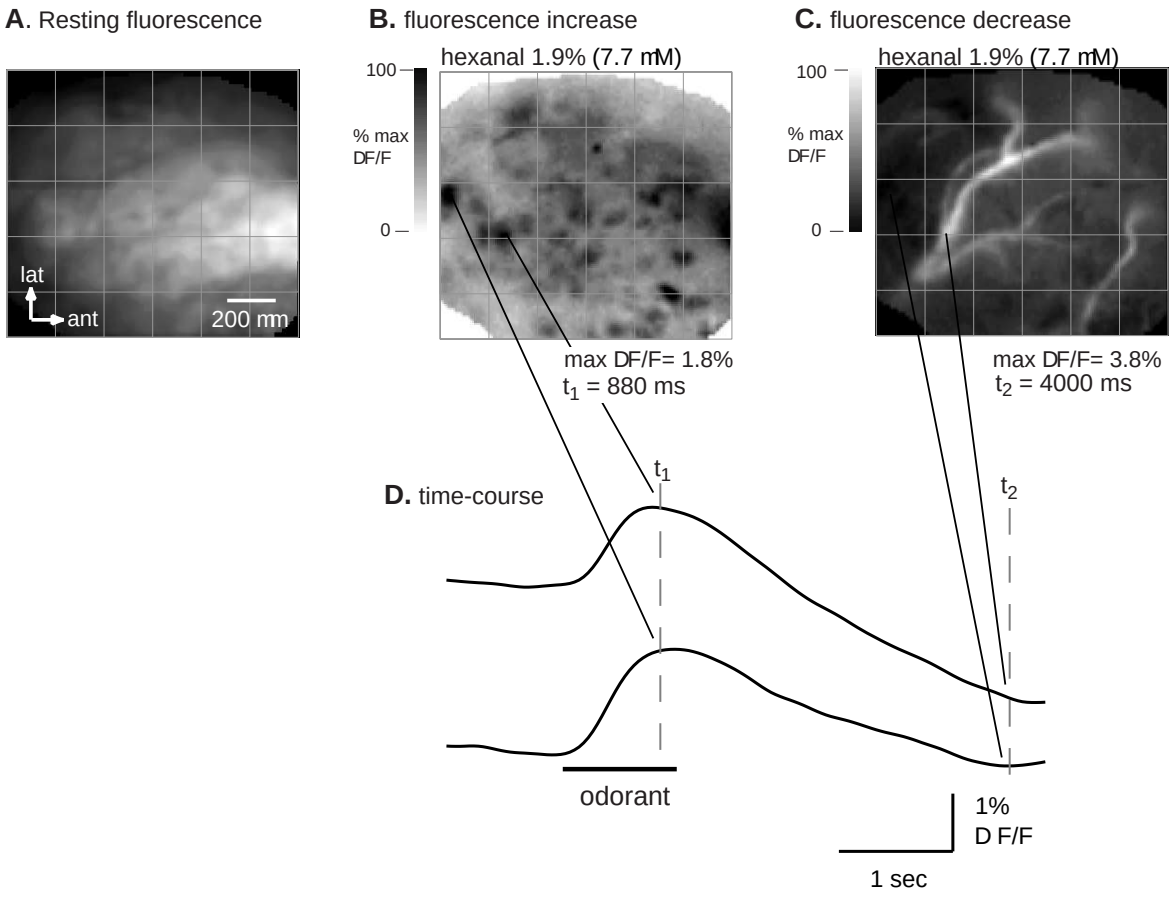

Supplemental figure
Wachowiak and Cohen